Near-field spectroscopy of porous silicon microcavity samples

F. Fuso,[a] M. Labardi, F. Sbrana,[b] L. Pardi, and M. Allegrini
INFM, Dipartimento di Fisica Enrico Fermi, Università di Pisa, Via F. Buonarroti 2, I-56127 Pisa, Italy

Z. Gaburro and L. Pavesi
INFM, Dipartimento di Fisica, Università di Trento, Via Sommarive 14, I-38050 Povo (Trento), Italy

(Received 22 March 2001; accepted for publication 22 January 2002)

Near-field optical spectroscopy has been used to investigate photoluminescence features of porous silicon microcavity samples with a subwavelength space resolution. The emission is found to be markedly dependent on the lateral position, with the presence of relatively narrow spectral features peaked at different wavelengths in the range 610–690 nm. Furthermore, the spectrum obtained by summing up spectra taken at different sampling points (relative displacement ~100 nm) recovers the standard (macroscopic) photoluminescence spectrum of porous silicon, except for the presence of a dip around the resonance wavelength of the microcavity resonator. © *2002 American Institute of Physics.* [DOI: 10.1063/1.1459747]

Near-field scanning optical microscopy (NSOM)[1] can be implemented to carry out near-field optical spectroscopy (NFOS) with a subwavelength space resolution, a technique particularly useful for light emitting samples. In this letter we report on NSOM/NFOS investigations on all-porous silicon (PSi) microcavities. In such samples photon confinement is exploited to improve the emission efficiency of the visible or near-IR through spatial rearrangement of the spontaneous emission. The luminescence is strongly peaked in the direction orthogonal to the microcavity surface,[2] opening the way for the development of novel interesting applications.[3–5]

Our NFOS investigation in air and at room temperature gives two major results. First, the well-known macroscopic photoluminescence (PL) in PSi is recovered by convolving spectral features of different small emitting centers randomly distributed on the sample surface. In this finding, which was not reported in previous near-field investigations on PSi,[6–8] the actual microcavity structure of the device is only accidentally involved. Our second finding suggests coupling between the optical near-field and the resonator structure. This is a not straightforward result due to the peculiar locality of the near-field irradiation by subwavelength apertures.

Our NSOM apparatus has been described in Refs. 9 and 10. Briefly, a commercial conically shaped tapered fiber tip (nominal aperture 50 nm, Al-coated taper) is used as a quasipoint-like emitter of light to locally excite the sample. In the present spectroscopic investigation, Ar^+ laser light at $\lambda_{exc}=458\,nm$ is coupled to the fiber tip. During the raster scan, the tip is approached at a constant distance (a few nm) to the sample by a distance regulation system, providing a topographic image of the surface. Emission is collected in the far field at 45° off surface by a long working-distance large-aperture microscope objective [Fig. 1(a)], and sent, through a multimode optical fiber, to a 240 mm monochromator equipped with a photomultiplier. Depending on the monochromator wavelength λ_{coll}, two different kinds of information can be acquired. If $\lambda_{coll}=\lambda_{exc}$, a near-field scattering map is obtained, i.e., a map of the local variations of intensity scattered by the sample surface, involving local modulations of its optical properties.[1] For emitting samples, by setting $\lambda_{coll}>\lambda_{exc}$ a near-field PL map is recorded. Furthermore, near-field PL spectra can be recorded by scanning the monochromator wavelength keeping the lateral position fixed. Signal detection is accomplished by optical chopping, low-noise current preamplification, and phase sensitive detection. The relatively low signal-to-noise (S/N) ratio of NFOS measurements imposes long integration times; typically, spectra in the full range of interest (610–690 nm) are acquired in 30–40 min.

The sample consists basically of a microcavity structure [see Fig. 1(a)] made of top and bottom symmetric mirrors enclosing a PSi layer in between.[3] Each mirror is made of 8+8 layers with alternate porosities (nominal refractive index for consecutive layers are 1.32 and 1.55), whereas the inner (''thick'') PSi layer has a nominal refractive index of 1.39. The starting Si wafer is of the p^+ type, and porosity and thickness of each layer are controlled during the growth by adjusting the anodization parameters. The optical thickness of the thick PSi layer is $\lambda_{cav}=676\,nm$, whereas that of the layers belonging to the top and bottom mirrors is chosen as $\lambda_{cav}/4$. Standard (i.e., macroscopic) PL for similar PSi microcavity samples has been widely studied,[2,3] showing a sharp emission peak located around λ_{cav} with a full width at half maximum (FWHM) ≈6 nm, for PL collected at the right angles. Correspondingly, reflectivity spectra at the right angles display a dip around λ_{cav}.

An example of results of our NSOM/NFOS analysis is presented in Fig. 1, where a comparison between topography (b), near-field scattering (c), and near-field emission at $\lambda_{coll}=650\,nm$ (d) images for the same portion of the sample is shown. Topography of the imaged region appears quite homogeneous, the average roughness being below 10 nm. On the right top corner, a portion of hill is seen, corresponding to

[a]Electronic mail: fuso@df.unipi.it
[b]Present address: DIBE, Università di Genova, I-16145 Genova, Italy.

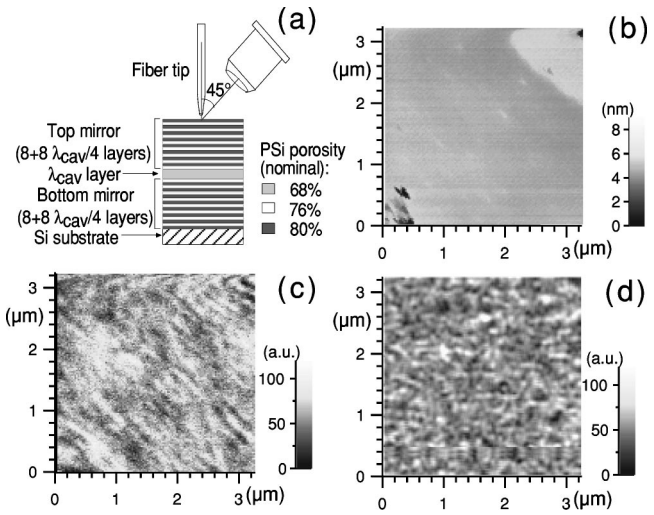

FIG. 1. Sketch of the experimental configuration and sample cross section (a); maps of topography (b), near-field scattering (c), and near-field emission at $\lambda_{coll}=650$ nm (d) for the same region of the sample.

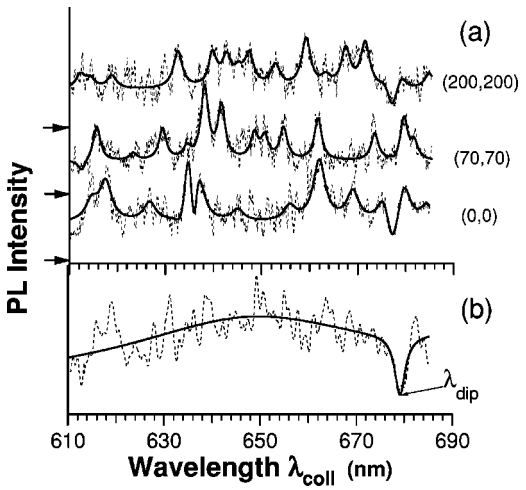

FIG. 2. Near-field PL spectra acquired at three different sampling positions (a), the relative displacement in nanometers along the in-plane directions being reported in brackets close to each trace. For the sake of clarity, spectra have been shifted vertically, the zero level for each spectrum being marked on the right axis by an arrow. Superimposed to experimental data (dotted lines) are the results of the fit (solid lines). PL spectrum obtained by summing up near-field spectra acquired at seven different fixed positions within a square with 700 nm lateral size (b). The solid line represents a guide for the eyes. The zero level corresponds to the horizontal axis.

the border of a protruding pore. Such a smooth surface, rather surprising in PSi, can be ascribed to the fabrication procedure, i.e., the multilayered structure and the use of a glycerol-based etching solution.[11] Many details are found in the near-field scattering map [Fig. 1(c)]. Features with a subwavelength average size are clearly visible, superimposed to traces of a periodic structure (average period $\sim\lambda_{exc}/2$) oriented approximately along the diagonal direction of the image. The pattern can be ascribed to interference effects following scattering at the interface between the uppermost layers of the microcavity structure. Indeed, the near-field produced by the tip is expected to illuminate the outer layer of the top mirror, since its subwavelength spatial extension is of the same order of magnitude of the layer thickness, or slightly larger. Other structures discerned in the scattering map, uncorrelated with the periodic pattern, can be due to local variations of the refractive index, as a consequence, for instance, of material oxidization. Also the emission map shows many different features; as an example, in Fig. 1(d), referring to a collection wavelength $\lambda_{coll}=650$ nm, small bright and dark spots are observed whose position is hardly correlated to the corresponding scattering image [Fig. 1(c)]. It must be noted that, in order to avoid thermal or mechanical drifts, the full image is acquired in a relatively short time (less than 60 min), so that the integration time available for each pixel is ~300 ms, leading to a poor S/N ratio. However, comparison between successively acquired images and, mostly, results of the spectral analysis presented in the following, suggest that the image shown actually represents a map of centers emitting at λ_{coll}. Line profile analysis shows that typical size of emitting centers is of the order of 100 nm (FWHM), or slightly larger. Maps acquired at different λ_{coll} also exhibit alternation of bright and dark spots, but with different space distributions.

Near-field excited radiation coming from different emitting centers has then been analyzed by acquiring near-field PL spectra at fixed sampling positions. An example of the results is shown in Fig. 2(a). Several features are observed above the noise level of the measurements; superimposed to experimental data a best-fit to multiple Lorentzian peaks is shown (solid lines). The best fit, reported only for the sake of clarity, has been performed by using a standard spectroscopic routine with the only constraint of a minimum peak width similar to the nominal wavelength resolution of our apparatus (~2 nm). No remarkable difference is observed when using Gaussian or Voigt fit functions. Peaks are present, centered at wavelengths dramatically depending on the sampling position. Also in this case, noise is relevant due to the weak near-field excitation. Measurement reliability has been assessed by carrying out different sets of measurements, and by checking that spectra acquired at the same sampling point are similar within the noise level of the experiment.

The occurrence of space-depending spectral features in PSi samples can be interpreted as due to local variations in both the size of Si nanocrystals involved in the emission mechanism and their environment (dangling bonds, passivation), expected to play a role in determining the spectral behavior. Our findings suggest a random space distribution of nanocrystals with different properties. By this assumption, we expect that the standard PL of PSi can be obtained as a convolution of spectral features pertaining to different emitting centers. By simply summing up near-field spectra acquired at seven fixed positions within a square of 700 nm lateral size, the spectrum displayed in Fig. 2(b) is obtained. This is similar to the room-temperature broad PL spectrum typical of nonstructured PSi samples. We note that, if single spectra were dominated by noise, no feature would be detected in the summed spectrum, which indirectly confirms the reliability of the emission measurements. As observed in other materials with an inhomogeneous space distribution of emitting centers,[12] NFOS allows us to interpret macroscopic features as due to the contribution of many different nano-

scopic space-resolved spectra. This point is in contradiction with previous near-field analyses of PSi samples,[8] where no remarkable difference was reported between near- and far-field spectral features, and the role of the chemical environment of Si nanocrystals was pointed out as the main one responsible in determining PL behavior. On the contrary, investigations on small emitting particles removed from PSi samples,[6] as well as on PSi particles with selected average size,[7] revealed a dependence of the peak wavelength on the sampling point, or on the sampled particle size, respectively. However, in no case has the presence of narrow spectral features been reported. Comparison with previous investigations suggests a great dependence of the results on the specific preparation procedures and properties of the sample under investigation. In particular, the presence of alternate thin PSi layers can contribute to the formation of relatively small regions containing Si nanocrystals with similar size and chemical environment. Moreover, the smooth surface of the sample is expected to favor a reliable mapping of the emitting centers. However, we cannot completely rule out a contribution from possible interference effects due to the multilayered structure of the sample.

A detailed inspection of near-field spectra reveals that emission at a wavelength λ_{dip}, slightly larger than the nominal resonant wavelength of the microcavity, is almost negligible independently of the sampling point, leading to the second result of our analysis. This circumstance is reflected in the appearance of a dip in the summed spectrum around 679 nm, not observed in far-field PL measurements at the right angles. This finding has no straightforward interpretation, but can be reasonably related to the presence of the microcavity structure.

The sharpness of the obtained dip ($\sim$2 nm FWHM) suggests that matching with the Bragg reflector refractive index is rapidly lost for inclined incidence. We infer that the radiation spontaneously emitted by the cavity top layer excited by the optical near field is preferentially directed at the right angles, due to the high density of photon states with wavelength λ_{cav}. The resonance condition is not so strong for the radiation that propagates at an angle θ with wavelength $\lambda_{cav}/\cos\theta$. Moreover, the larger the incidence angle, the larger the area of the microcavity sample concerned by the multiple reflections (scaling as $\tan^2\theta$), and thus the stronger the role of refractive index inhomogeneities, that the NSOM images have shown to occur on the μm scale [see Fig. 1(c)]. Conversely, the resonance condition for light propagating at the right angle is the best defined one, since radiation propagation involves smaller, and thus more homogeneous, cavity regions.

The localized excitation provided by near-field tapered probes gives evidence of the cavity effect in ruling the spontaneous emission of PSi nanocrystals. Hence, a dip appears for inclined collection, possibly due to depletion of emitted photons in the direction of the optical detector at 45°. Point-like excitation (in both depth and lateral size) provides a clearly defined resonance condition for the locally emitted photons, inducing a dip sharper than the macroscopic emission width, with a slightly different wavelength due to the local resonance condition occurring at the investigated site. The sharp dip is not observable in macroscopic (far-field) experiments, due to the full illumination of the cavity structure, that may lead to compensation effects between the emission from layers belonging to symmetrically opposite Bragg reflectors, and to local inhomogeneities of the cavity refractive index.

In conclusion, the peculiar excitation features accessible by near-field optical microscopy are an interesting prospect for the coupling of light sources to microoptical devices.

L. C. Andreani is gratefully acknowledged for enlightening discussions. The work has been carried out within Progetto Finalizzato MADESS II (subproject ''Diodi elettroluminescenti a base di Si-poroso'') of the Italian National Research Council (CNR).

[1] E. Betzig and J. K. Trautman, Science **257**, 189 (1992).
[2] V. Pellegrini, A. Tredicucci, C. Mazzoleni, and L. Pavesi, Phys. Rev. B **52**, R14328 (1995).
[3] L. Pavesi, Riv. Nuovo Cimento **20**, 1 (1997).
[4] S. Chan and P. M. Fauchet, Appl. Phys. Lett. **75**, 274 (1999).
[5] V. Mulloni and L. Pavesi, Appl. Phys. Lett. **76**, 2523 (2000).
[6] J. K. Rogers, F. Seiferth, and M. Vaez-Iravani, Appl. Phys. Lett. **66**, 3260 (1995).
[7] M. D. Mason, G. M. Credo, K. D. Weston, and S. K. Buratto, Phys. Rev. Lett. **80**, 5405 (1998).
[8] P. J. Moyer, T. L. Cloninger, J. L. Gole, and L. A. Bottomley, Phys. Rev. B **60**, 4889 (1999).
[9] P. G. Gucciardi, M. Labardi, S. Gennai, F. Lazzeri, and M. Allegrini, Rev. Sci. Instrum. **68**, 3088 (1997).
[10] M. Labardi, P. G. Gucciardi, and M. Allegrini, Riv. Nuovo Cimento **23**, 4 (2000).
[11] V. Mulloni, C. Mazzoleni, and L. Pavesi, Semicond. Sci. Technol. **14**, 1052 (1999).
[12] R. Cingolani, G. Bastard, M. Labardi, F. Fuso, M. Allegrini, L. Sorba, L. Vanzetti, and A. Franciosi, J. Appl. Phys. **86**, 6793 (1999).